The 3rd International Conference on Structural Health Monitoring of Intelligent Infrastructure
Vancouver, British Columbia, Canada
November 13-16, 2007

DEVELOPMENT AND CHARACTERIZATION OF A SMART FRP PATCH WITH EMBEDDED FBG SENSOR FOR STRAIN MONITORING OF RC STRUCTURES

P. Corvaglia
Consorzio CETMA, Italy

A. Largo
Consorzio CETMA, Italy

M.A. Caponero
ENEA, Italy

L. Fiori
ENEA, Italy

Abstract

Optical fibers sensor, serving as both sensor and data conduit, are particularly interesting for the long-term health monitoring of civil structures. Nevertheless, many challenges associated with the on-the-field application of such sensors have to be solved, mainly related to the application methodology and the long-term properties under severe environmental conditions.

In this paper, the development and validation of smart composite patches (SPs), composed of FRP (Fiber Reinforced Plastic) reinforcing sheets with embedded FBG (Fiber Bragg Grating) optical sensors is presented. Tensile tests were carried out, comparing the strain measures from the FBG sensors to data obtained from electrical strain gauges in order to calibrate the transfer function of the SP, which can also have a reinforcing function.
The SPs were then mounted on a batch of both FRP-reinforced and un-reinforced r.c. elements, that were tested in flexure in order to evaluate the correct strain transfer from the structure to the patch and to investigate on the possible stiffening effects introduced by the patch on the structure to be monitored. Moreover, some specimens were exposed to different environmental conditions for a long-term evaluation. The in-situ validation of the new sensor is scheduled to be held on a highway r.c. bridge structure.

INTRODUCTION

Optical fibers, serving as both sensor and data conduit, are particularly interesting for the structural health monitoring of civil structures; among optical fiber sensors, FBG (Fiber Bragg Grating) sensors have gained numerous applications, being durable, stable and insensitive to external electromagnetic and environmental perturbations. Nevertheless, many challenges associated with their use in real-world cases have not yet been solved, mainly related to the application methodology and the long-term properties under severe environmental conditions.
In this paper, the development and validation of smart composite patches (SPs) is presented, in which the FBG sensor is pre-packaged, by manual lay-up combined with vacuum bagging technique, in a thin composite tape, that can than be easily mounted on the structure to be monitored. The pre-package gives the optical fiber the necessary protection against an accidental damaging during handling and installation, so making them as easy to handle as

other traditional strain gauges (SG), allowing, at the same time, the reinforcing of the existing structure and the real-time remote monitoring of the strain status. In a previous stage of the research (Corvaglia et al., 2005) the authors verified that the presence of the FBG sensor inside the FRP does not cause any significant reduction in the longitudinal tensile mechanical properties of the SP (fabricated by only manual wet lay-up) so evidencing that the new sensor can be used for strengthening purpose as well. The obtained results suggested investigating on a more quality-controlled manufacturing method, aiming at a reduction of the properties scattering. After the calibration of the transfer function the SPs were mounted on a batch of concrete elements (some of them reinforced with FRPs, some with steel rebars, some with both reinforcements), that were tested in flexure in order to evaluate the correct strain transfer from the structure to the SP and to investigate on the possible stiffening effects introduced by the SP on the structure to be monitored. Moreover, some specimens were exposed to different environmental conditions in order to evaluate the long-term properties. The in-situ validation of the new sensor is finally scheduled to be held on a highway r.c. bridge structure.

MAIN PRINCIPLES OF FIBER BRAGG GRATING (FBG) SENSORS

Typically, an FBG sensor consists of a single mode fiber with a short length grating written within the core. If a broadband light signal is traveling into the fiber, the grating acts as a filter, reflecting only the light component at the specific wavelength called λ_{Bragg}. When the FBG is strained a shift of the reflection spectrum can be observed. The theoretical wavelength shift for isothermal conditions is given by (Davis et al., 1997):

$$\frac{\Delta\lambda_{Bragg}}{\lambda_{Bragg}} = (1 - p_e)\varepsilon \tag{1}$$

where ε is the strain over the sensor length and p_e is the effective photoelastic constant for the fiber (approximately 0.22 for silica glass). Comprehensive reviews of the fundamentals of FBG sensors are given in the literature (Hill et al., 1997; Bennion et al., 1996).

SPECIMEN CONFIGURATION AND PREPARATION

The SPs were produced using the hand lay – up and vacuum bagging technique, embedding the optical fiber between two plies of GFRP fabric (0.3 mm thick, 425 g/m^2 heavy, with a weft/warp ratio of 1.15) impregnated with epoxy resin. A new tensile specimen configuration (Figure 1) was set-up, where the fiber is embedded only in the central region of the sample, in order to avoid possible damage or signal loss due to the gripping force of the tensile test machine during the characterization stage.

Figure 1. Manufacturing of SPs for SHM

Five samples of this kind of SPs (FBG Series) were produced in order to demonstrate feasibility, to test the quality of bonding between the optical fiber and the surrounding FRP structure, and to determine the mechanical and optical performances. Moreover, forty SPs with the optical fiber embedded along the overall length of the laminate were manufactured for the flexure tests on concrete beams.

SMART PATCH CALIBRATION

Embedding FBG sensors in FRP materials could alter their photoelastic constant with the consequent need of SP calibration, that was performed by means of a tensile test, according to the ASTM D3039 standard. Each specimen (FBG series) was instrumented with both FBG sensor and traditional SG, in order to verify that the strain was properly transferred from the FRP host structure to the FBG sensor. Since all experiments were conducted in temperature controlled environment, the thermal effect could be neglected in the study. Linearity of the $\Delta\lambda$ - ε relationship was evaluated by verifying the ratio between $\Delta\lambda$ measured by the FBG sensor and the patch strain ε, measured by the SG, was constant during the test (a typical calibration curve is shown in Figure 2). Once verified linearity, the transfer function was defined for each specimen through the calculation of the slope of the $\Delta\lambda$ - ε experimental curve and expressed in the form of eq. 1 (Table 1). An average transfer function was then defined using the mean calculated value of p_e.

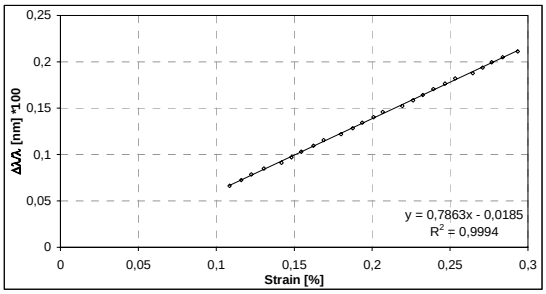

Figure 2. Linearity evaluation for FBG 1 specimen

Table 1. Calibration for FBG batch

Specimen	p_e
FBG 1	0,21
FBG 2	0,17
FBG 3	0,21
FBG 4	0,22
FBG 5	0,17
Average Value	0,20
Coeff. of variation [%]	2,86

CYCLIC TENSILE TEST

Three SPs were subjected also to cyclic tensile loads (10 cycles from 800 N to 1660 N, cross-head speed of 0,3 mm/min); strain was calculated with the average transfer function defined above. A typical strain – time curve is reported, as a reference, in Figure 3: the strains measured from the electrical SG and from the SP are compared and a very good agreement is observed (superimposed curves), for low cycles number at least.

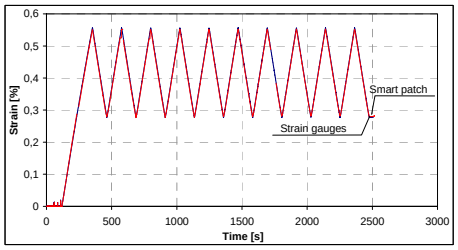

Figure 3. Strain – time curve for cyclic tensile tests

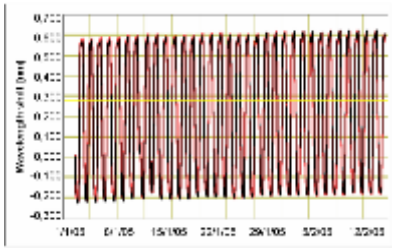

Figure 4. Ageing tests results

AGEING TESTS

Several SPs, some of which mounted on concrete specimens, were subjected to ageing tests by hydro-thermal cycling (table 2).

Table 2. Ageing tests parameters

Test duration	Cycles duration	Temperature range	Relative humidity range
8 months	24 hours	-10°C to +40°C	0% to 90%

A reference wavelength shift – time curve, referred to a 30 days period, is shown in Figure 4. It can be pointed out that the SP correctly follow the deformation induced on the concrete specimens by the hydro-thermal cycling so evidencing that the structural contact does not decay. The slight drift toward higher average wavelength shift can be accounted for by a residual deformation of the concrete mainly due to the humidity absorption. The alteration of the periodic cycling occurring in two consecutive days is due to the opening of the door of the environmental chamber for service. In Figure5 the morphology of the fiber-resin interface of a SP is showed. A SEM inspection of several cross-sections showed that a uniform and smooth acrylate – resin interface is present after the cycling period and no structural adhesion decay is observed.

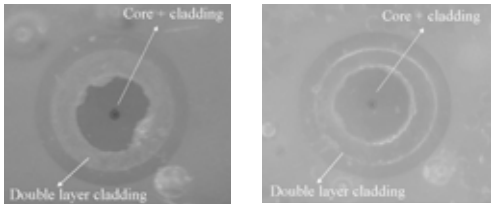

Figure5: SEM analysis of the morphology of the fiber-resin interface
(left: reference, right: after 2 months ageing)

FLEXURE TESTS

Specimens preparation and instrumentation

A total of six plain concrete beams and six steel-reinforced concrete beams were manufactured. For each of the two series, three specimens were strengthened using externally bonded CFRP sheets.

Table 3. Tested beam types (3 samples for each type)

Label	Beam type
CSP	Concrete beams with SP
RCSP	Reinforced concrete beams with SP
CFSP	FRP reinforced concrete beams with SP
RCFSP	FRP and steel reinforced concrete beams with SP

All beams were tested in four-point bending; the strain distribution was measured by five strain gauges in tension (SG) and three in compressions (SG c), serving as reference data. SPs were also bonded on the tension surface of the CSP, CFSP and RCSP specimens (the system used to label these beams is reported in Table 3); two SPs (one on the tension surface, the other on the compression surface (SPc)) were mounted on the RCFSP specimens (Figure 6). Flexural tests were then performed in order to evaluate the correct strain transfer from the host structure to the SP bonded on different substrates. One of the primary objectives of this study is to assess how reliably the SP can read strain near and during concrete failure and to evaluate the advantages of using embedded sensors rather than surface attached SGs.

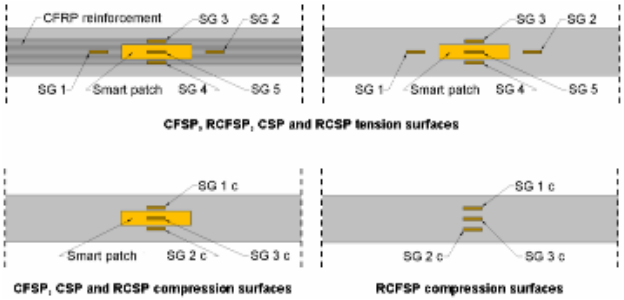

Figure 6. Details of specimen's instrumentation

RESULTS: CFSP SERIES

The tensile strain – time curves of the CFSP series specimens are shown in Figure 7; the strains measured from the electrical SGs and from the SP are compared and a good agreement is observed. Data scattering increases at a certain load level, after the beginning of concrete cracking, but the scattering is not only between the SP data and the mean SGs data, but also among the single SGs data.

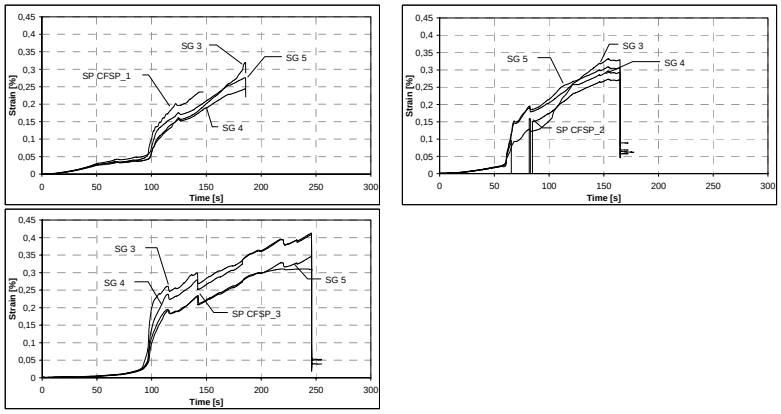

Figure 7. Tensile strain – time curves of the CFSP series specimens

RESULTS: RCFSP SERIES

The strain – time curves of the RCFSP series specimens are shown in Figure 8.

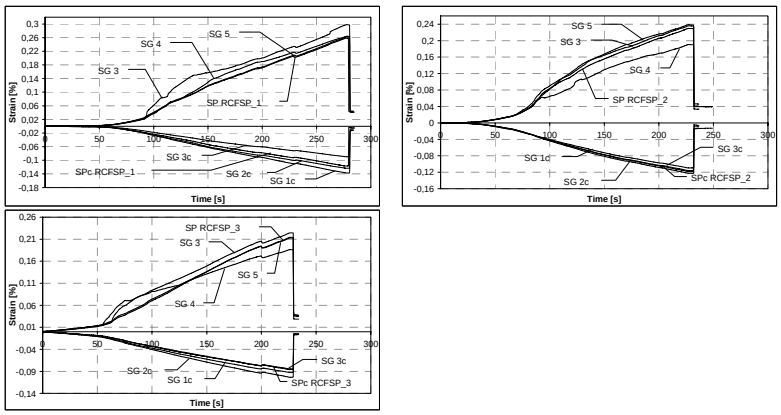

Figure 8. Tensile and compressive strain – time curves of the RCFSP series specimens

For this kind of specimens two SPs, each one with different λ_{Bragg}, were mounted (one on the tension surface, the other on the compressive surface) and serially multiplexed. SG 3c is the SG mounted on the SP on the compression surface. Also in this case a very good agreement is obtained both in tension and in compression. The observed good agreement with the strain measured by the SG 3c gives a positive indication that the photoelastic constant obtained in tension tests can be used for the compression case as well.

RESULTS: CSP SERIES

The tensile strain – time curves of the CSP series specimens are shown in Figure 9; again, a good agreement can be pointed out. Due to an improper data recording of the opto – electronic unit, it was not possible to obtain the tensile strain – time curve for the CSP 2 specimen.

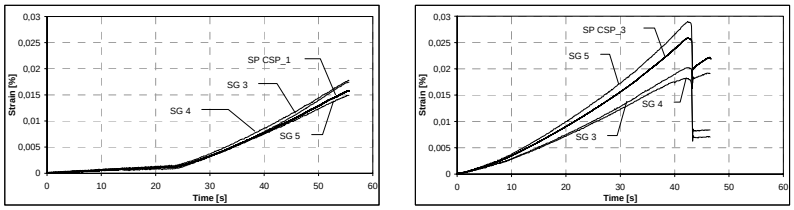

Figure 9 Tensile strain – time curves for CSP series specimens

RESULTS: RCSP SERIES

The tensile strain – time curves of the RCSP series specimens are shown in Figure 10. A quite good agreement is obtained, although, unlike the previous tests, for these specimens the difference between the SP and SGs measured strain is more evident. This is probably mainly due to the irregular and porous concrete surface that could have caused an improper bonding of the sensors (SP and SGs) to the substrate. Finally, the SP on the RCSP 2 specimen was mounted by means of a quick setting epoxy resin, in order to evaluate the possible use of this kind of adhesive for in – situ installations; on the basis of the obtained results it can be thought that it does not allow a proper strain transfer from the host structure to the patch.

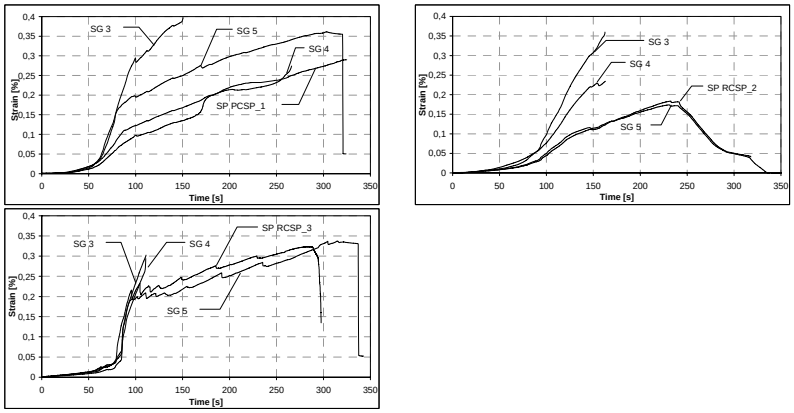

Figure 10 Tensile strain – time curves for RCSP series specimens

RESULTS: ANALYSIS OF THE STIFFENING EFFECT OF THE SMART PATCHES

The reinforcing effect of SPs mounted on r.c. and concrete beams, also reinforced with CFRP sheets, was evaluated by comparing the slope of the load – midspan deflection curves for specimens with similar geometrical and mechanical properties with and without SP (Table 4). Such evaluation is important in order to estimate the possible error induced by the sensor on the magnitude of the parameters to be measured. Although the observed values are, in these cases, not small, the stiffening effect will decrease passing to the application on real-case structures, having bigger cross-section and steel rebar reinforcement.

Table 4. Reinforcement effect evaluation (Δ is the percentage stiffness increase due to the presence of the SP)

	Not externally reinforced	FRP externally reinforced
r.c. beams	$\Delta = 10$ %	$\Delta = 11$ %
plain concrete beams	$\Delta = 21$ %	$\Delta = 29$ %

DYNAMIC TESTS

A structural model constituted by a plane beam-column joint reinforced with FRP sheets, was realized and subjected to shaking table tests (Figure 11 (a)) using an artificial accelerogram compatible with the spectrum provided by the Italian OPCM 3431/2005 for the zone named 3 and the soil type named C. Two SPs were symmetrical mounted at the base of the first level column, in order to measure axial deformations; a reference SG was also mounted close to each SP. A typical strain – time curve is reported, as an example, in Figure 11 (c): the strains measured from the electrical SG and from the SP are compared and a very good agreement is observed (superimposed curves).

(a)

(b)

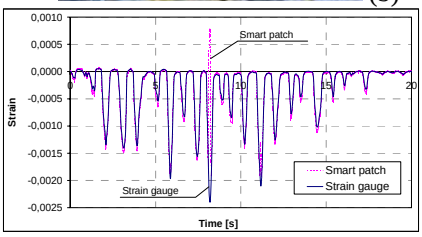

(c)

Figure 11. Structural model (a); SP installation (b); Strain – time curves (c)

REAL CASE STUDY

The in-situ validation of the new sensor is being carried out on a highway RC single span bridge structure, in the framework of the seismic upgrade intervention on the bridge by means of FRP materials.

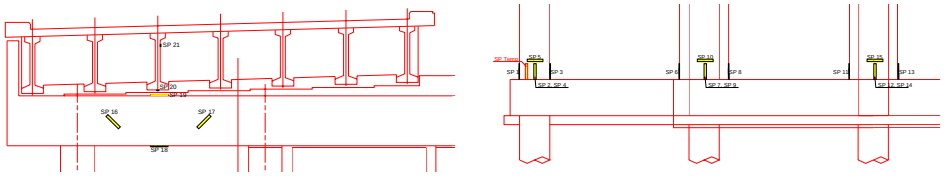

Figure 12. SPs positioning for SHM of a highway RC bridge

Twenty-two SPs are being installed in the positions described in Figure 12, in order to continuously monitor the deformation status of the structure. As the bridge is symmetrical designed, only half of the structure is instrumented.

CONCLUSIONS

The article presents the development and validation of a smart FRP patch, in which an FBG sensor is pre-packaged, using a manual lay-up combined with vacuum bagging technique, in a thin composite plate. This can then be easily mounted on the structure to be monitored; also allowing its reinforcement.

After the calibration of the transfer function, the SP was installed on a batch of both FRP – reinforced and un – reinforced r.c. elements, that were tested in flexure in order to evaluate the correct strain transfer from the structure to the SP and to investigate on the possible stiffening effects introduced by the SP on the structure to be monitored. From the experimental results, a good agreement was observed between the strain measured by the SP and by traditional SGs, also mounted on the specimens, both in tension and in compression; moreover the observed stiffening effect of SPs, although not negligible, will decrease passing to the application on real-case structures, having bigger cross-section and steel rebar reinforcement.

The ageing tests evidenced no performances decay after hydro-thermal cycling. The new sensor was finally validated in dynamic tests performed on a r.c. structural model reinforced with FRP sheets.

The good results obtained in lab tests allow the conclusion that the SP is a good candidate to replace standard electrical SG for SHM monitoring of civil structures.

The in-situ validation of the new sensor is being carried out on a highway r.c. single span bridge structure, in the framework of the seismic upgrade intervention on the bridge by means of FRP materials.

REFERENCES

1. Corvaglia, P., Largo, A., Caponero, M.A., Colonna, D. and Fiori, L. (2005), “Development of smart composite patch with embedded FBG sensor for real – time monitoring of civil structures”, *Proceedings of Advancing with Composites, Naples, Italy*.
2. Corvaglia, P., Largo, A., Caponero, M.A., Fiori, F. (2006), “Real - time monitoring of r.c. elements by means of smart composite patches with embedded FBG sensor”, *Proceedings of Structural faults + Repair 2006, Edinburgh, Scotland*.
3. Davis, M.A., Bellemore, D.G., and A.D., Kersey (1997) “Distributed fiber Bragg grating strain sensing in reinforced concrete structural components”, *Cement and concrete composites*, Vol. 19, published by Elsevier.
4. Hill, K.O. and Meltz, G. (1997) “Fiber Bragg grating technology fundamentals and overview”, *Journal of Lightwave Technology*, Vol. 15.
5. Bennion, I., Williams, J.A.R., Zhang, L., Sugden, K. and Doran, N.J. (1996) “UV written in-fiber Bragg gratings”, *Optical and Quantum Electronics*, Vol. 28.